To appear in The Astronomical Journal
Preprint typeset using LaTeX style emulateapj v. 10/09/06

HIPPARCOS ASTROMETRIC ORBIT AND EVOLUTIONARY STATUS OF HR 6046

Guillermo Torres
Harvard-Smithsonian Center for Astrophysics, 60 Garden St., Cambridge, MA 02138
Draft version February 1, 2008

ABSTRACT

The previously known, 6-yr spectroscopic binary HR 6046 has been speculated in the past to contain a compact object as the secondary. A recent study has re-determined the orbit with great accuracy, and shown that the companion is an evolved but otherwise normal star of nearly identical mass as the primary, which is also a giant. The binary motion was detected by the *Hipparcos* mission but was not properly accounted for in the published astrometric solution. Here we use the *Hipparcos* intermediate data in combination with the spectroscopic results to revise that solution and establish the orbital inclination angle for the first time, and with it the absolute masses $M_{\rm A} = 1.38^{+0.09}_{-0.03}$ M$_\odot$ and $M_{\rm B} = 1.36^{+0.07}_{-0.02}$ M$_\odot$. Aided by other constraints, we investigate the evolutionary status and confirm that the primary star is approaching the tip of the red-giant branch, while the secondary is beginning its first ascent.

Subject headings: astrometry — binaries: general — binaries: spectroscopic — methods: data analysis — stars: fundamental parameters — stars: individual (HR 6046)

1. INTRODUCTION

Since the publication of the first preliminary orbits in the 1930's by Christie (1934, 1936), the bright giant star HR 6046 (HD 145849, HIP 79358, $\alpha = 16^{\rm h}11^{\rm m}48\overset{\rm s}{.}05$, $\delta = +36°25'30\overset{''}{.}3$, J2000.0; spectral type K3 II, $V = 5.63$) has been known as a highly eccentric ∼6-yr period single-lined spectroscopic binary of particular interest. The relatively large minimum mass inferred early on for the companion (> 3 M$_\odot$), along with the fact that it was not visible to early observers, led to the speculation that the secondary was a collapsed star (Trimble & Thorne 1969), more commonly referred to nowadays as a black hole. Very recently Scarfe et al. (2007) have dispelled this notion by detecting the secondary spectroscopically and showing that it is merely an evolved late-type star, with nothing particularly out of the ordinary in its properties other than the fact that it is faint. On the basis of extensive radial velocity measurements carried out over more than 26 years these authors presented an accurate double-lined orbit for the system yielding minimum masses considerably smaller than previously thought. They also found the components to be nearly identical in mass to within about 1%, even though they are substantially different in brightness ($\Delta V \approx 3$). They relied on the *Hipparcos* parallax of the system (Perryman et al. 1997) to construct a plausible photometric model of the stars (individual magnitudes and colors), but cautioned that the distance could be vitiated by unmodeled photocentric motion.

As described by Scarfe et al. (2007), HR 6046 has never been spatially resolved despite repeated attempts over the years using speckle interferometry and other techniques. However, Jancart et al. (2005) were able to obtain an estimate of the inclination angle by reconsidering the *Hipparcos* Intermediate Astrometric Data in conjunction with the spectroscopic orbit of Christie (1936) to account for the binary motion. With this the absolute masses of the components can in principle be obtained, although the resulting values are somewhat high for late-type giants (∼3.6 M$_\odot$) possibly because of the use of outdated spectroscopic elements.

The main motivation for the present work is to revisit the *Hipparcos* astrometric solution in the light of the accurate orbit of Scarfe et al. (2007), and to examine the effect on the published parallax. Additionally, we investigate the evolutionary status of the system with our newly determined masses, aided by current stellar evolution models. We report also a spectroscopic determination of the effective temperature of the primary star that supports the general picture outlined by other constraints in showing the evolved state of the binary.

2. HIPPARCOS OBSERVATIONS AND REVISED ASTROMETRIC SOLUTION

Given the 6-yr orbital period of HR 6046, which is of the same order as the duration of the *Hipparcos* mission (slightly more than 3 yr), it may be expected that the orbital motion would be detectable in the satellite measurements, and that if not properly accounted for, it could bias either the trigonometric parallax, the proper motions, or both. Indeed, proof that a signal of this nature is detectable is given by the fact that the *Hipparcos* team found it necessary to include acceleration terms in the astrometric solution, representing the first derivatives of the proper motions. These terms, $d\mu^*_\alpha/dt = -9.08 \pm 1.23$ mas yr^{-2} and $d\mu_\delta/dt = -6.98 \pm 1.53$ mas yr^{-2}, are statistically significant. It is unclear why a full orbital model was not applied originally to this system, since the binary nature of the object has been known for a long time. In any case, this has been done more recently by Jancart et al. (2005), as mentioned earlier.

A total of 78 astrometric measurements were made by *Hipparcos* from 1989 December to 1993 February, covering about 53% of an orbital cycle. Each measurement consisted of a one-dimensional position ('abscissa', v) along a great circle representing the scanning direction of the satellite, tied to an absolute frame of reference known as the International Celestial Reference Sys-

Electronic address: gtorres@cfa.harvard.edu

tem (ICRS). The measurements available for our analysis are published in the form of 'abscissa residuals' (Δv; see Table 1), which are the residuals from the standard five-parameter solution reported in the Catalogue (Perryman et al. 1997). The five standard parameters are the position (α_0^*, δ_0) and proper motion components (μ_α^*, μ_δ) of the barycenter at the reference epoch 1991.25[1], and the trigonometric parallax, $\pi_{\rm t}$. The nominal errors of these measurements have a median value of 2.5 mas.

We incorporated orbital motion into a new astrometric solution following the formalism of van Leeuwen & Evans (1998), Pourbaix & Jorissen (2000), and Jancart et al. (2005), including the correlations between measurements from the two independent data reduction consortia that processed the original *Hipparcos* observations (NDAC and FAST; Perryman et al. 1997). Details of this modeling along with another example of an application may also be seen in Torres (2007b). In the most general case the adjustable quantities of the fit (a total of 12) are the corrections to the five standard *Hipparcos* parameters ($\Delta\alpha^*$, $\Delta\delta$, $\Delta\mu_\alpha^*$, $\Delta\mu_\delta$, and $\Delta\pi_{\rm t}$), and the seven usual elements of the binary orbit: the period P, the semimajor axis of the photocenter $a_{\rm phot}$, the eccentricity e, the inclination angle i, the longitude of periastron for the primary $\omega_{\rm A}$, the position angle of the ascending node Ω (equinox J2000.0), and the time of periastron passage T. For HR 6046 the *Hipparcos* measurements do not constrain P, e, $\omega_{\rm A}$, or T sufficiently well, so those elements were held fixed at their spectroscopic values as reported by Scarfe et al. (2007). We solved for the remaining 8 parameters simultaneously using standard non-linear least-squares techniques (Press et al. 1992, p. 650). The reduced χ^2 of the solution is 0.9895, indicating that the internal errors of the abscissa residuals are realistic.

We list the results in Table 2, where they are compared with those obtained by Jancart et al. (2005). Significant differences are seen in the semimajor axis and inclination angle, which reflect the spectroscopic constraints used in each case. Jancart's value of $a_{\rm phot}$ is nearly twice as large as ours, and while their inclination angle is substantially smaller than 90°, we obtain an orientation that is essentially edge-on. The smaller i value of Jancart et al. (2005) would lead to much larger absolute masses for the stars when combined with the minimum masses of Scarfe et al. (2007), as noted in §1. There is little doubt that the recent orbital elements by Scarfe et al. (2007) supersede the provisional values of Christie (1936) adopted by Jancart, which suggests our solution should be closer to the truth.[2] An external check on our results is provided by the absolute proper motions we obtain, listed in the bottom section of Table 2. These are different from the values reported in the *Hipparcos* Catalogue, which are likely to be affected also by the unmodeled orbital motion. They agree well, however, with the motions given in the Tycho-2 Catalogue (Høg et al. 2000), as shown in Table 3. The latter are based on the position from the Tycho experiment aboard the *Hipparcos* satellite (epoch ∼1991.25) combined with ground base catalog positions going back nearly a century in some cases. This long baseline tends to average out any orbital motion that has a period of a few years, as in the case of HR 6046, and therefore yields a more accurate estimate than *Hipparcos*. Finally, we note that our revised *Hipparcos* solution did not change the value of the parallax significantly, which was one of the concerns of Scarfe et al. (2007). This parallax corresponds to a distance of 178 pc.

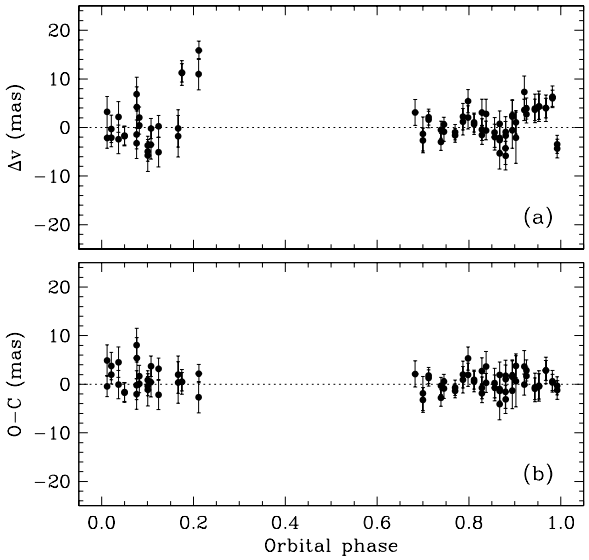

FIG. 1.— (a) Abscissa residuals of HR 6046 from the *Hipparcos* mission as a function of orbital phase. These are the residuals from the standard 5-parameter solution as published in the Catalogue (Perryman et al. 1997). The systematic patterns are due to the unmodeled motion of the center of light. (b) $O-C$ residuals of the *Hipparcos* measurements from our new 12-parameter fit that accounts for the orbital motion.

As a way of visualizing the effect of accounting for the orbital motion in the *Hipparcos* solution, we show in Figure 1a the abscissa residuals Δv resulting from the standard 5-parameter solution as a function of orbital phase. Some systematic patterns are apparent, but they largely disappear after the orbital motion is incorporated into the model. This is shown by the O–C residuals from the 12-parameter fit in Figure 1b.

The projection of the photocentric orbit on the plane of the sky along with a schematic representation the *Hipparcos* measurements is seen in Figure 2, where the axes are parallel to the right ascension and declination directions. Because these measurements are one-dimensional in nature, their exact location on the plane of the sky cannot be shown graphically. The filled circles represent the predicted location on the computed orbit (see also Figure 3). The dotted lines connected to each filled circle indicate the scanning direction of the *Hipparcos* satellite for each measurement, and show which side of the orbit the residual is on. The length of each dotted line represents the magnitude of the $O-C$ residual.[3]

[1] Following the practice in the *Hipparcos* Catalogue we define $\alpha^* \equiv \alpha\cos\delta$ and $\mu_\alpha^* \equiv \mu_\alpha\cos\delta$.

[2] A preliminary version of the Scarfe et al. (2007) work had been published in 2004 (Scarfe et al. 2004), but was perhaps not yet available to Jancart and collaborators.

[3] The "$O-C$ residuals" are not to be confused with the "abscissa residuals" Δv, which we refer to loosely here as *Hipparcos* "observations" or "measurements". As indicated earlier, the abscissa residuals are in fact residuals from the standard 5-parameter fit reported in the *Hipparcos* Catalogue, whereas the $O-C$ residu-

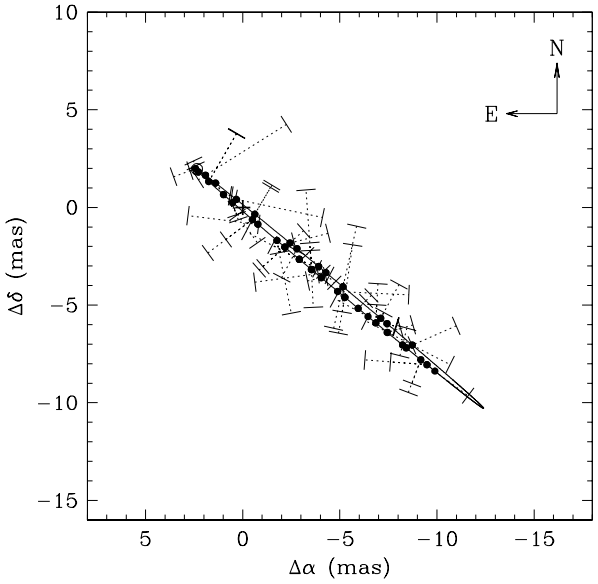

FIG. 2.— Motion of the photocenter of HR 6046 relative to the center of mass of the binary (indicated by the plus sign) as seen by *Hipparcos*. The one-dimensional abscissa residuals are shown schematically with a filled circle at the predicted location, dotted lines representing the scanning direction of the satellite, and short perpendicular line segments indicating the undetermined location of the measurement on that line (see text). The length of the dotted lines represents the magnitude of the $O-C$ residual from the computed location. Three measurements with residuals larger than 5 mas were omitted for clarity. Also indicated on the plot is the location of periastron (open circle near the top).

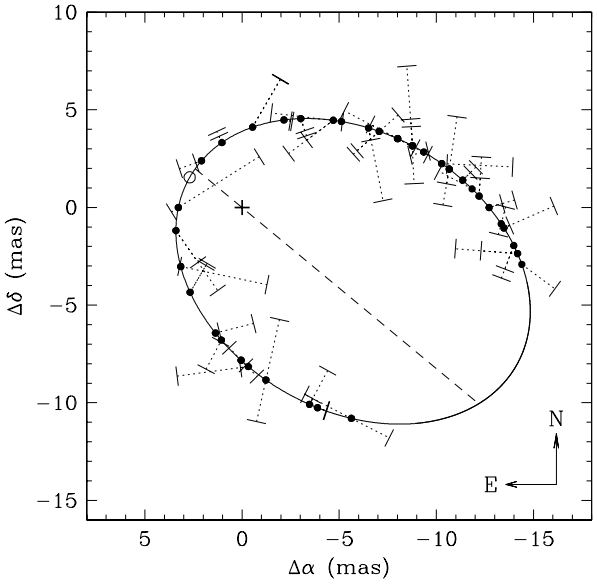

FIG. 3.— Same as Figure 2, except that the orbit has been deprojected to appear as if it were viewed exactly face-on. The line of nodes is indicated with the dashed line. Motion on the plane of the sky in this figure is direct (counterclockwise).

The short line segments at the end of and perpendicular to the dotted lines indicate the direction along which the actual observation lies, although the precise location is undetermined. Occasionally more than one measurement was taken along the same scanning direction, in which case two or more short line segments appear on the same dotted lines. The orbit is formally clockwise (retrograde), although the orientation is so close to edge-on ($i = 91\overset{\circ}{.}4 \pm 9\overset{\circ}{.}7$) that the motion on the plane of the sky may well be direct.

The phase coverage of the *Hipparcos* observations is seen more clearly in Figure 3, in which we have deprojected the orbit and represented it as if it were viewed with an inclination angle of 0°. The measurements happen to cover the periastron passage of 1991.83 (indicated with an open circle), but not apastron. The path of HR 6046 on the plane of the sky as seen by *Hipparcos* is shown in Figure 4. The irregular pattern is the result of the combination of annual proper motion (indicated by the arrow), parallactic motion, and orbital motion.

The detection of the photocentric motion by *Hipparcos* offers an independent way of estimating the brightness difference between the stars, in the passband of the satellite (H_p band), from the relation between the semi-major axis of the photocentric orbit and that of the relative orbit in angular units (e.g., van de Kamp 1967): $a_{\rm phot} = a_{\rm rel}(B-\beta)$. Here $a_{\rm rel}$ can be obtained from the spectroscopic minimum masses, the inclination angle, and the parallax through Kepler's Third Law. B represents the mass fraction $M_{\rm B}/(M_{\rm A}+M_{\rm B})$, and β is the

als (or simply "residuals") are the difference between the abscissa residuals and the computed position of the star from a model that incorporates orbital elements.

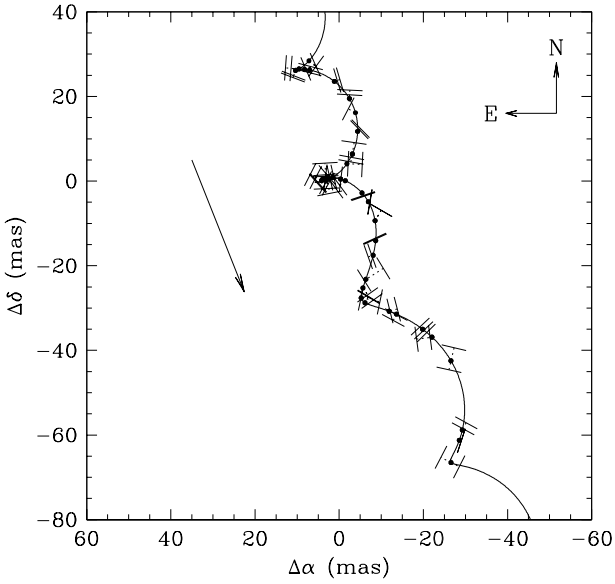

FIG. 4.— Path of the center of light of HR 6046 on the plane of the sky, along with the *Hipparcos* observations (abscissa residuals) represented as in Figure 2 and Figure 3. The irregular motion is the result of the combined effects of the annual parallax, proper motion, and orbital motion according to the solution described in the text. The arrow indicates the direction and magnitude of the annual proper motion.

light fraction given by $L_{\rm B}/(L_{\rm A}+L_{\rm B}) = (1+10^{0.4\Delta H_p})^{-1}$. The magnitude difference is then

$$\Delta H_p = 2.5 \log \left[\left(\frac{q}{1+q} - \frac{a_{\rm phot}}{a_{\rm rel}} \right)^{-1} - 1 \right] , \qquad (1)$$

in which $q \equiv M_{\rm B}/M_{\rm A}$. We obtain $\Delta H_p = 2.1 \pm 0.6$ mag, somewhat smaller but still broadly consistent with the values in the Johnson B and V bands reported by Scarfe et al. (2007) (see below), considering the difference in the passbands.

3. EVOLUTIONARY STATUS

From the analysis of their high-resolution spectra of HR 6046 Scarfe et al. (2007) estimated the spectral types and luminosity classes of the components to be K3 II and K0 IV, and the brightness difference to be $\Delta B \approx 2.5$ mag and $\Delta V \approx 3.0$ mag. They then made use of the *Hipparcos* parallax (which we now know is substantially correct) and the combined system brightness to infer absolute visual magnitudes of $M_V = -0.68$ for the primary and $M_V = 2.32$ for the secondary, ignoring extinction. $U-B$ and $B-V$ color indices were computed by making use of standard tabulated values for spectral types and luminosity classes close to what they derived, along with the magnitude differences. The photometry synthesized in this way provides a very good match to the observed *B–V* color of the system, and enabled Scarfe et al. (2007) to claim that both stars are evolved, with the primary being near the tip of the giant branch. They also pointed out that evolutionary models by Pols et al. (1998) allow the brightness difference to be as large as observed in HR 6046 for component masses that differ by as little as they do in this system (∼1%), at least for masses in the most probable range for HR 6046, which they estimated to be 2.0–3.5 $M_\odot$. This provided a natural explanation for a set of properties that had intrigued earlier investigators.

The minimum masses from the spectroscopic work of Scarfe et al. (2007) combined with our inclination angle give absolute masses for HR 6046 of $M_{\rm A} = 1.38^{+0.09}_{-0.03}$ $M_\odot$ and $M_{\rm B} = 1.36^{+0.07}_{-0.02}$ $M_\odot$ (Table 2), in which the uncertainties are currently dominated by the error in i. These masses are considerably smaller than assumed by those authors. We have therefore re-examined the consistency with the evolutionary models by making use of these values along with slightly revised absolute magnitudes for the stars based on our new parallax. Given a distance approaching 200 pc, a small amount of extinction would not be unexpected for the system, and in fact the dust maps of Schlegel et al. (1998) indicate a total reddening in the direction of HR 6046 of $E(B-V) \sim 0.03$ mag. We tentatively adopt $E(B-V) \sim 0.02 \pm 0.01$ mag, which corresponds to $A_V \sim 0.06 \pm 0.03$ mag. With this adjustment to the apparent magnitude $V = 5.63 \pm 0.01$ (Häggkvist & Oja 1987), and taking into account the magnitude difference from Scarfe et al. (2007) (to which we assign, somewhat arbitrarily, an uncertainty of 0.3 mag), we infer individual magnitudes of $M_V^{\rm A} = -0.62 \pm 0.20$ and $M_V^{\rm B} = 2.38 \pm 0.34$. These are not changed much from the original estimates of Scarfe et al. (2007). The $B-V$ colors proposed by them rely on an external tabulation and are quite sensitive to the luminosity class adopted, so we have preferred to proceed without them here, although they may well be accurate. The models by Girardi et al. (2000) are a convenient choice for a comparison with the observations, since they reach the late evolutionary stages needed for the primary and are tabulated for a wide range of chemical compositions and ages. They also incorporate mass loss due to winds in the giant phase, which turns out to be only a 1–2% effect for HR 6046.

In Figure 5 we show several isochrones for different metallicities from this series of models that produce the best simultaneous match to the absolute magnitudes of both components at their current masses (accounting for mass loss). In each case (except for the middle isochrone) the age is the one providing the best agreement among the values tabulated by Girardi et al. (2000), which come in steps of 0.05 in $\log t$. The location of the stars on these models is indicated with open circles. The combined color and magnitude predicted for the system in each case is shown by the plus signs, and the filled circle represents the measured values of M_V and *B–V* for HR 6046. The system color we have adopted is $B-V = 1.34 \pm 0.01$ (Häggkvist & Oja 1987), which we have then dereddened as indicated above. Properties of the stars inferred from these models are listed in Table 4. If we now impose the additional requirement that the isochrones match the measured system color within its uncertainty, a very good correspondence may be obtained by interpolation for a metallicity of $Z = 0.011 \pm 0.002$ (corresponding to [Fe/H] $= -0.24 \pm 0.07$ for the assumed $Z_\odot = 0.019$ in these models) and a logarithmic age of $\log t = 9.49^{+0.04}_{-0.09}$ (or $3.1^{+0.3}_{-0.6}$ Gyr). This model is shown with the heavy line in Figure 5, and indicates that the primary is indeed approaching the tip of the giant branch, whereas the secondary is beginning its first ascent of the giant branch. We infer from this best-fitting isochrone that the primary star has a radius of $30.9^{+3.6}_{-1.1}$ $R_\odot$, a surface gravity of $\log g = 1.60^{+0.04}_{-0.08}$, and an effective temperature ($T_{\rm eff}$) of 4211^{+16}_{-23} K, and the secondary has $R = 4.20^{+0.27}_{-0.33}$ $R_\odot$, $\log g = 3.33^{+0.07}_{-0.04}$, and $T_{\rm eff} = 5010^{+79}_{-47}$ K. These uncertainties account for all observational errors but exclude possible systematics in the models. Other properties of the stars for this metallicity are listed in Table 4.

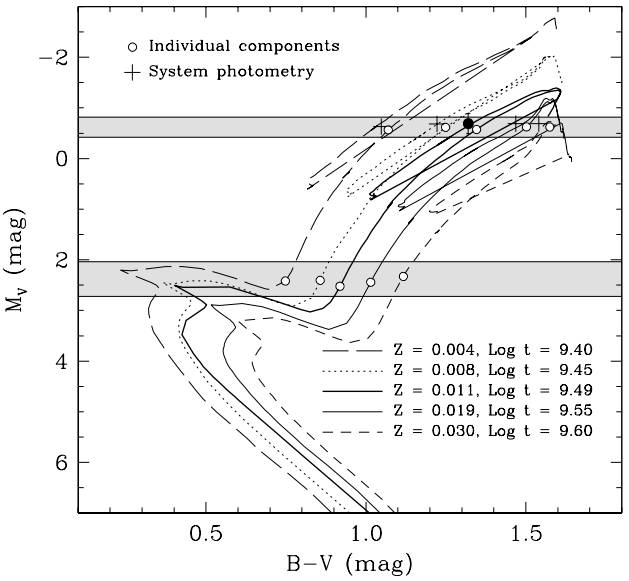

FIG. 5.— Model isochrones from Girardi et al. (2000) that match the measured absolute magnitudes (grey areas) and current masses of HR 6046 within the observational errors, shown for a range of metallicities and ages as labeled. Open circles on each isochrone indicate the expected location of the components, and the plus signs represent the predicted system magnitude and color. The system magnitude and color actually measured are represented by the filled circle and error bar. The model drawn with the heavy line satisfies the additional constraint given by the observed $B-V$ color of the system.

3.1. *Additional spectroscopic constraints*

With the goal of providing a check on the temperature of the primary star, we obtained a high-resolution spectrum of HR 6046 on UT 5 July 2007 using the HIRES instrument (Vogt et al. 1994) on the Keck I telescope. The spectrometer slit was $0\farcs86$, giving a resolving power of $\lambda/\Delta\lambda \approx 55{,}000$. The signal-to-noise ratio of this spectrum is ∼120 per pixel. The spectral region $\lambda\lambda$6200–6300 Å was used to measure a number of temperature-sensitive lines mainly of Fe I and V I, and also a few of Ni I, Sc I, Si I, and Fe II. As described by Gray & Johanson (1991) and others, line-depth ratios (LDRs) of properly selected line pairs are an excellent diagnostic of effective temperature that allow for *relative* measurements with a precision as small as a few K, not only in dwarfs but also in giants (Gray & Brown 2001). The conversion to an *absolute* temperature scale, however, necessarily depends on an external color-temperature calibration since LDR variations are usually compared with corresponding changes in a color index such as $B{-}V$, which is an easier quantity to measure than temperature. Therefore, absolute temperatures are much less certain. We measured a total of 26 lines of the primary star[4] from Table 1 by Biazzo et al. (2007), and used their calibrations appropriate for giants for 16 selected line pairs to derive an average temperature from the LDRs of $T_{\rm eff} = 4340 \pm 20$ K (formal error). The scatter of the individual determinations is only 80 K. The color-temperature relation on which the above calibrations are based is that of Gray (2005), which combines dwarf and giant temperatures obtained by many different methods. For this work we have preferred to rely on a more sophisticated color-temperature relation such as that by Ramírez & Meléndez (2005), which accounts not only for luminosity class but also metallicity, and is based on effective temperatures derived homogeneously by the Infrared Flux Method. The conversion from the above LDR-based $T_{\rm eff}$ back to an average color for the primary star was made using the same prescription by Gray (2005), and gives $B-V = 1.328 \pm 0.014$. The Ramírez & Meléndez (2005) calibration for an adopted metallicity of [Fe/H] = −0.24 (§3) then yields $T_{\rm eff} = 4210 \pm 60$ K, in which the error combines photometric uncertainties and the scatter of the calibration. This result is in virtually perfect agreement with the temperature predicted by the Girardi et al. (2000) models, supporting our overall conclusions from the previous section.

4. DISCUSSION AND CONCLUDING REMARKS

The example of HR 6046 is one of a growing number of binaries in which the *Hipparcos* intermediate data have been brought to bear on the orbit of the system, providing complementary information to that afforded by other types of observations (see, e.g., Pourbaix et al. 2004; Fekel et al. 2005, 2007; Torres 2006, 2007a,b). In this case the *Hipparcos* data yield the inclination angle, and allow the absolute masses to be derived for the first time. Additionally they provide an estimate of the brightness difference.

Although the inclination we derive for the orbit is consistent with 90° and allows for the possibility of eclipses, chances are slim because of the long period compounded by the relatively large uncertainty in i. No photometric variability was found by Percy (1993), who, however, apparently did not observe during the eclipse phases, or by the *Hipparcos* satellite (scatter $\sigma_{H_p} = 0.007$ mag). The latter observations do straddle two of the eclipses, which can be predicted very accurately from the spectroscopic orbit of Scarfe et al. (2007) with errors of only 1.0 days for primary eclipse (HJD 2,448,652.4) and 1.4 days for the secondary (HJD 2,448,419.3). If central, the eclipses would last approximately 18 and 22 days, respectively. Examination of the epoch photometry from *Hipparcos* indicates that both of these eclipses were missed by just a few days. Future eclipses would be expected to occur at Julian dates $2{,}455{,}254.7 \pm 1.2$ and $2{,}457{,}455.5 \pm 1.4$ for the primary, and $2{,}455{,}021.6 \pm 1.4$ and $2{,}457{,}222.4 \pm 1.6$ for the secondary. The small separation of only 233 days (10.6% of a cycle) between the secondary eclipses and the primary events that follow is due to a combination of high eccentricity and a longitude of periastron near zero.

A second implication of the near edge-on orientation of HR 6046 is significantly lower component masses than previously assumed, which in turn leads to a linear semi-major axis for the relative orbit of 4.63 ± 0.11 AU, corresponding to 26.0 ± 2.4 mas. The maximum angular separation subtended by the binary is about 43 mas, also considerably smaller than has been suggested in the past (∼70 mas; McAlister 1976; Halbwachs 1981). About two dozen unsuccessful attempts to detect the secondary have been made over the past 3 decades with the speckle technique. Some of them were made at phases in the orbit when the instrumental resolution should have allowed the observers to resolve the pair, suggesting the large disparity in brightness ($\Delta V \approx 3$) as the cause of those non-detections. In principle the expected separations make it a good target for long-baseline interferometry, except that in most cases these instruments observe in the near infrared, where the brightness difference will be even more extreme. From our modeling we expect $\Delta J \sim 3.8$ mag and $\Delta K \sim 4.1$ mag. Still, some of these facilities may have the sensitivity required. They could also resolve the primary itself; the angular diameter should be approximately 1.6 mas, while that of the secondary is only 0.2 mas.

Double-lined spectroscopic binaries with two giant components are a relatively rare occurrence, and usually imply the components must have nearly identical mass. HR 6046 is quite remarkable in that the stars have attained a large brightness difference that is near the maximum for this system, yet the secondary is still visible. Evolution proceeds very rapidly at this stage, and according to the models the difference in brightness may still increase by another half a magnitude or so in V over the next 20 Myr, which represents only ∼0.5% of its present age.

We are grateful to an anonymous referee for helpful suggestions on the original manuscript. Partial support for this work from NSF grant AST-0708229 and NASA's MASSIF SIM Key Project (BLF57-04) are acknowledged. This research has made use of the VizieR service (Ochsenbein et al. 2000) and of the SIMBAD

[4] The secondary is too faint to affect these measurements, and would not influence them even if it were brighter (see Gray & Brown 2001).

database, both operated at CDS, Strasbourg, France, as well as of NASA's Astrophysics Data System Abstract Service. Alex Sozzetti is thanked for help in obtaining and reducing the Keck spectrum of HR 6046.

REFERENCES

Biazzo, K., Frasca, A., Catalano, S., & Marilli, E. 2007, Astr. Nach., in press
Christie, W. H., 1934, PASP, 46, 238
Christie, W. H., 1936, ApJ, 83, 433
Fekel, F. C., Barlow, D. J., Scarfe, C. D., Jancart, S., & Pourbaix, D. 2005, AJ, 129, 1001
Fekel, F. C., Williamson, M., & Pourbaix, D. 2007, AJ, 133, 2431
Girardi, L., Bressan, A., Bertelli, G., & Chiosi, C. 2000, A&AS, 141, 371
Gray, D. F. 2005, The Observation and Analysis of Stellar Photospheres, 3rd Edition, Cambridge, UK: Cambridge University Press
Gray, D. F., & Brown, K. 2001, PASP, 113, 723
Gray, D. F., & Johanson, H. L. 1991, PASP, 103, 439
Häggkvist, L., & Oja, T. 1987, A&AS, 68, 259
Halbwachs, J.-L. 1981, A&AS, 44, 47
Høg, E., Fabricius, C., Makarov, V. V., Urban, S., Corbin, T., Wycoff, G., Bastian, U., Schwekendiek, P., & Wicenec, A. 2000, A&A, 355, L27
Jancart, S., Jorissen, A., Babusiaux, C., & Pourbaix, D. 2005, A&A, 442, 365
McAlister, H. A. 1976, PASP, 88, 317
Ochsenbein, F., Bauer, P., & Marcout, J. 2000, A&AS, 143, 23
Percy, J. R. 1993, PASP, 105, 1422
Perryman, M. A. C., et al. 1997, The *Hipparcos* and Tycho Catalogues (ESA SP-1200; Noordwjik: ESA)
Pols, O. R., Schröder, K.-P., Hurley, J. R., Tout, C. A., & Eggleton, P. P. 1998, MNRAS, 298, 525
Press, W. H., Teukolsky, S. A., Vetterling, W. T., & Flannery, B. P. 1992, Numerical Recipes, (2nd. ed.; Cambridge: Cambridge Univ. Press)
Pourbaix, D., & Jorissen, A. 2000, A&AS, 145, 161
Pourbaix, D., Jancart, S., & Jorissen, A. 2004, in Spectroscopically and Spatially Resolving the Components of the Close Binary Stars, ASP Conf. Ser. 318, eds. R. W. Hilditch, H. Hensberge & K. Pavlovski (San Francisco: ASP, p. 144
Ramírez, I., & Meléndez, J. 2005, ApJ, 626, 465
Scarfe, C. D., Griffin, R. F., & Griffin, R. E. M. 2004, Rev. Mexicana Astron. Astrofís, 21, 79
Scarfe, C. D., Griffin, R. F., & Griffin, R. E. M. 2007, MNRAS, 376, 1671
Schlegel, D. J., Finkbeiner, D. P., & Davis, M. 1998, ApJ, 500, 525
Torres, G. 2006, AJ, 131, 1022
Torres, G. 2007a, ApJ, 654, 1095
Torres, G. 2007b, AJ, 133, 2684
Trimble, V. L., & Thorne, K. S. 1969, ApJ, 156, 1013
van de Kamp, P. 1967, Principles of Astrometry (San Francisco: W. H. Freeman)
van Leeuwen, F., & Evans, D. W. 1998, A&AS, 130, 157
Vogt, S. S. et al. 1994, Proc. SPIE, 2198, 362

TABLE 1
Hipparcos Intermediate Astrometric Data for HR 6046.

Date (HJD−2,400,000)	Year	Orbital Phase	Δv (mas)	$\sigma_{\Delta v}$ (mas)	$O-C$ (mas)	Consortium (NDAC/FAST)
47862.0382	1989.9165	0.6830	+3.09	2.68	+2.12	N
47899.4398	1990.0187	0.6999	−1.33	3.49	−1.89	F
47899.4398	1990.0189	0.7000	−2.65	2.55	−3.21	N
47926.5048	1990.0931	0.7123	+2.13	1.65	+1.79	F
47926.5048	1990.0930	0.7123	+1.63	1.69	+1.29	N
47985.6022	1990.2552	0.7392	−0.49	1.76	−0.33	F
47985.6022	1990.2549	0.7392	−2.97	1.71	−2.81	N
47999.3721	1990.2924	0.7454	−0.85	2.00	−0.89	F
47999.2991	1990.2924	0.7454	+0.61	1.47	+0.57	N
48053.5022	1990.4408	0.7700	−0.96	1.57	−0.71	F
48053.5022	1990.4408	0.7700	−1.62	1.43	−1.37	N
48091.2325	1990.5437	0.7871	+1.17	2.71	+0.93	F
48091.2325	1990.5432	0.7870	+2.25	2.73	+2.01	N
48115.2294	1990.6101	0.7981	+5.42	2.38	+5.31	F
48115.2294	1990.6098	0.7981	+2.05	2.39	+1.94	N
48144.5225	1990.6901	0.8114	+1.04	1.94	+0.95	F
48144.5225	1990.6901	0.8114	+0.65	2.09	+0.56	N
48181.7780	1990.7918	0.8283	+3.07	2.74	+2.72	N
48182.2163	1990.7932	0.8285	−1.53	1.94	−1.86	F
48182.2163	1990.7935	0.8285	−0.43	2.22	−0.76	N
48201.2823	1990.8454	0.8372	−0.61	1.93	+0.28	F
48201.2823	1990.8454	0.8372	+2.77	3.06	+3.66	N
48243.0304	1990.9602	0.8562	−1.98	2.67	−0.73	F
48243.0304	1990.9598	0.8561	−1.02	3.05	+0.23	N
48266.5891	1991.0237	0.8667	−2.61	2.89	−1.37	F
48266.5525	1991.0243	0.8668	−5.34	3.20	−4.09	N
48267.0273	1991.0245	0.8669	−2.19	2.50	−0.98	F
48266.9908	1991.0245	0.8669	+0.73	2.67	+1.94	N
48294.9690	1991.1022	0.8798	−5.80	2.92	−3.10	F
48294.9690	1991.1019	0.8797	−4.27	3.35	−1.58	N
48295.4073	1991.1027	0.8799	−1.66	2.89	+1.04	F
48295.4073	1991.1031	0.8799	−0.94	3.18	+1.76	N
48327.3666	1991.1911	0.8945	+2.25	3.32	+1.51	F
48327.3666	1991.1906	0.8944	−0.54	3.72	−1.28	N
48327.8050	1991.1918	0.8946	+2.48	3.24	+1.77	N
48344.7526	1991.2382	0.9023	+1.05	2.43	+3.80	F
48344.6795	1991.2378	0.9023	−2.10	5.27	+0.63	N
48384.6744	1991.3475	0.9205	+3.62	2.18	−0.05	F
48384.6744	1991.3475	0.9205	+7.30	3.27	+3.63	N
48395.7049	1991.3779	0.9255	+2.72	1.82	+1.70	F
48395.7049	1991.3777	0.9255	+3.88	2.17	+2.86	N

TABLE 1 — *Continued*

Date (HJD−2,400,000)	Year	Orbital Phase	Δv (mas)	$\sigma_{\Delta v}$ (mas)	$O-C$ (mas)	Consortium (NDAC/FAST)
48436.1381	1991.4882	0.9438	+3.63	2.22	−0.93	F
48436.1016	1991.4884	0.9439	+3.91	2.95	−0.65	N
48455.2042	1991.5408	0.9526	+4.28	2.58	−0.43	F
48455.2042	1991.5406	0.9525	+4.37	3.14	−0.34	N
48488.4784	1991.6314	0.9676	+4.01	2.03	+2.86	F
48488.4419	1991.6316	0.9676	+3.98	2.72	+2.83	N
48519.9995	1991.7182	0.9820	+6.03	1.68	+0.35	F
48519.9995	1991.7180	0.9820	+6.31	2.24	+0.62	N
48543.0468	1991.7812	0.9925	−4.35	1.92	−1.21	F
48543.0468	1991.7811	0.9924	−3.45	1.85	−0.31	N
48586.1097	1991.8990	0.0120	−2.14	2.13	−0.43	F
48586.1097	1991.8990	0.0120	+3.20	3.17	+4.91	N
48606.0524	1991.9536	0.0211	−2.08	1.91	+1.98	F
48606.0524	1991.9537	0.0211	−0.31	2.82	+3.75	N
48640.2398	1992.0469	0.0366	−2.43	2.93	−0.06	F
48640.2033	1992.0471	0.0366	+2.16	3.14	+4.53	N
48669.0580	1992.1261	0.0497	−1.67	1.95	−1.60	F
48669.0580	1992.1261	0.0497	−1.80	2.00	−1.73	N
48727.5346	1992.2865	0.0763	−1.45	2.97	−0.21	F
48727.5346	1992.2862	0.0763	−3.25	3.14	−2.02	N
48728.0459	1992.2872	0.0764	+6.85	3.47	+8.06	F
48728.0094	1992.2875	0.0765	+4.19	4.20	+5.40	N
48739.9896	1992.3200	0.0819	+0.44	1.82	+0.09	F
48739.9896	1992.3202	0.0819	+2.03	2.19	+1.68	N
48780.7880	1992.4323	0.1005	−4.94	1.99	−0.37	F
48780.7880	1992.4320	0.1005	−3.69	1.90	+0.87	N
48781.2263	1992.4333	0.1007	−5.75	3.30	−1.15	N
48795.8728	1992.4736	0.1074	−0.22	2.09	+3.70	F
48795.8728	1992.4733	0.1073	−3.51	3.01	+0.41	N
48832.2517	1992.5731	0.1239	+0.26	2.23	+3.18	F
48832.2517	1992.5725	0.1238	−5.10	3.03	−2.18	N
48926.3036	1992.8306	0.1666	−0.19	3.83	+1.97	F
48926.3036	1992.8304	0.1666	−1.81	4.28	+0.34	N
48944.4931	1992.8802	0.1749	+11.27	1.89	+0.50	F
48944.4931	1992.8801	0.1748	+11.24	2.54	+0.47	N
49025.1768	1993.1013	0.2116	+15.87	1.89	+2.19	F
49025.1768	1993.1011	0.2115	+10.99	3.22	−2.69	N

TABLE 2
ASTROMETRIC ORBITAL SOLUTIONS FOR HR 6046.

Parameter	Jancart et al. (2005)[a]	This work[b]
Adjusted quantities		
P (days)	2150 (fixed)	2200.77 (fixed)
$a_{\rm phot}$ (mas)	16.5 ± 2.3	9.69 ± 0.85
e	0.6 (fixed)	0.6797 (fixed)
i (deg)	46.4 ± 3.5	91.4 ± 9.7
$\omega_{\rm A}$ (deg)	340 (fixed)	9.73 (fixed)
$\Omega_{\rm J2000}$ (deg)	305.4 ± 6.7	50.5 ± 6.6
T (HJD−2,400,000)	50699 (fixed)[c]	50760.4 (fixed)
$\Delta\alpha^*$ (mas)	···	+4.41 ± 0.76
$\Delta\delta$ (mas)	···	+3.77 ± 0.95
$\Delta\mu_\alpha^*$ (mas yr^{-1})	···	−3.57 ± 0.91
$\Delta\mu_\delta$ (mas yr^{-1})	···	−3.13 ± 1.23
$\Delta\pi_{\rm t}$ (mas)	···	+0.27 ± 0.51
Derived quantities		
μ_α^* (mas yr^{-1})	···	−12.46 ± 0.91
μ_δ (mas yr^{-1})	···	−31.13 ± 1.23
$\pi_{\rm t}$ (mas)	···	5.61 ± 0.51
$M_{\rm A}$ ($M_\odot$)	···	$1.38^{+0.09}_{-0.03}$
$M_{\rm B}$ ($M_\odot$)	···	$1.36^{+0.07}_{-0.02}$

[a] P, e, $\omega_{\rm A}$, and T adopted from Christie (1936). Other *Hipparcos*-related parameters were not reported.[b] P, e, $\omega_{\rm A}$, and T adopted from Scarfe et al. (2007).[c] Projected forward from the original epoch 2,424,290 (HJD) using the more accurate period from the present paper, for easier comparison with our new results.

TABLE 3
Comparison of the proper motion and parallax results for HR 6046.

Parameter	*Hipparcos*	Tycho-2	This paper
μ_α^* (mas yr^{-1})	-8.89 ± 0.58	-13.3 ± 1.4	-12.46 ± 0.91
μ_δ (mas yr^{-1}).....	-28.00 ± 0.60	-30.8 ± 1.4	-31.13 ± 1.23
$\pi_{\rm t}$ (mas)	5.34 ± 0.60	···	5.61 ± 0.51

TABLE 4
Properties for the components of HR 6046 inferred from the models.

Property	$Z = 0.004$	$Z = 0.008$	$Z = 0.011$	$Z = 0.019$	$Z = 0.030$
Log age (yr)	9.40	9.45	9.49	9.55	9.60
$(B-V)_{\rm A}$ (mag).....	1.07	1.25	1.35	1.50	1.58
$(B-V)_{\rm B}$ (mag).....	0.75	0.87	0.92	1.02	1.12
$(B-V)_{\rm tot}$ (mag).....	1.05	1.22	1.32	1.47	1.54
ΔJ (mag).....	3.48	3.64	3.80	3.96	4.11
ΔH (mag).....	3.66	3.88	4.05	4.29	4.43
ΔK (mag).....	3.68	3.90	4.08	4.33	4.54
$T_{\rm eff}^{\rm A}$ (K).....	4590	4311	4211	3947	3699
$T_{\rm eff}^{\rm B}$ (K).....	5312	5079	5010	4819	4649
$R_{\rm A}$ ($R_\odot$).....	23.1	29.3	30.9	42.1	56.7
$R_{\rm B}$ ($R_\odot$).....	3.84	4.33	4.20	4.98	5.90

Note. — The models used are those of Girardi et al. (2000), and the observational constraints are the measured masses and absolute magnitudes of the components (see text). The best-fitting model for $Z = 0.011$ satisfies the additional constraint that the combined colors of the components match the observed $B-V$ color.